Improved Differential and Linear Cryptanalysis on Round-Reduced SIMON

Chao Niu, Muzhou Li, Jifu Zhang, and Meiqin Wang(✉)

Abstract—SIMON is a lightweight block cipher proposed by the National Security Agency. According to previous cryptanalytic results on SIMON, differential and linear cryptanalysis are the two most effective attacks on it. Usually, there are many trails sharing the same input and output differences (resp. masks). These trails comprise the differential (resp. linear hull) and can be used together when mounting attacks. In ASIACRYPT 2021, Leurent *et al.* proposed a matrix-based method on SIMON-like ciphers, where only trails whose active bits stay in a w-bit window are considered. The static window in each round is chosen to be w least significant bits. They applied this efficient framework on SIMON and SIMECK, and have obtained many better differentials and linear hulls than before. For SIMON, they also found that there seems to be some potential for improvement, which should be further investigated.

In this paper, we dynamically choose window for each round to achieve better distinguishers. Benefiting from these dynamic windows, we can obtain stronger differentials and linear hulls than previously proposed for almost all versions of SIMON. Finally, we provided the best differential/linear attacks on SIMON48, SIMON64, and SIMON96 in terms of round number, complexity, or success rate.

Index Terms—SIMON, Dynamic Window, Differential Attack, Linear Attack.

1 Introduction

The SIMON [1] cipher is a suite of lightweight block ciphers proposed by the National Security Agency in 2013. Due to its simple round function and good performance in hardware and software, SIMON has gained a lot of attention since its proposal. It follows a Feistel structure with a very simple round function:

$$f(x) = (\mathrm{S}^8(x) \wedge \mathrm{S}^1(x)) \oplus \mathrm{S}^2(x),$$

where $\mathrm{S}^a(x)$ denotes the a-bit left cyclic rotation of x.

Previous cryptanalytic results show that the best attacks on it use differential cryptanalysis or linear cryptanalysis [2], [3], [4], [5], [6], [7], [8]. Meanwhile, there can be many trails in a differential or a linear hull that could be used to mount attacks together. However, the expected probability of the differential (EDP) and the expected linear potential (ELP) of the linear hull are both hard to evaluate due to the massive amount of trails comprising them.

In ASIACRYPT 2021, Leurent *et al.* [9] proposed a novel framework to deal with this for SIMON-like ciphers, where only trails whose input differences stay in the least w significant bits in each round are considered. In this paper, we refer to it as the w-bit *static window* (SW). Unlike previous methods to enumerate the good trails contributing to the differential or the linear hull, they efficiently compute the probability distribution by multiplication of the differential transition matrix or linear correlation matrix round by round, which can consider *all* trails with active bits staying in the w-bit SW. Using this method, they found longer distinguishers that are more conducive to key recovery attacks and improved the previous best attack for several rounds for both SIMON and SIMECK [10].

1.1 Motivations and Contributions.

To include as many good trails as possible, Leurent *et al.* [9] adopted the same w-bit SW for all rounds. In other words, the diffusion of the included input and output differences (resp. masks) for each round are restricted. The SW is chosen to contain the least significant bits. With the increase of the window size w, the results obtained with SW will gradually approach the lower bounds of EDP and ELP. Eventually, they will become stable. Of course, the bigger w leads to a tighter lower bound of EDP and ELP. However, the size of window w is restricted by the memory size of the computer resources one can exploit. In [9], the maximum of w is 19 and the matrix size will be $2^{19\times 2}$ as the memory size for their used computer is 1TB. They claimed that the ELP for SIMON could not get stable when the window size w is even set to be 19, while both EDP and ELP for SIMECK could. By confining the active bits to the w least significant bits window, the static window strategy constructs a differential transition or linear correlation matrix that contains *all* trails only with active bits in the fixed window for each round. In other words, the static window strategy discards all trails with active bits out of the w least significant bits window. Compared with SIMECK, SIMON has a stronger diffusion property due to the bigger rotation constant. It means that the static window strategy may lose some good trails even in the first few rounds for SIMON. Therefore, choosing a flexible window for each round can avoid losing too many trails and lead to better distinguishers. However, how to choose these windows for SIMON is an interesting problem. In this paper, we focus on this problem and propose the

- *Chao Niu, Muzhou Li, Jifu Zhang and Meiqin Wang are with Key Laboratory of Cryptologic Technology and Information Security, Ministry of Education, Shandong University, Jinan, China, and also with School of Cyber Science and Technology, Shandong University, Qingdao, China. E-mail: niuchao, muzhouli, zhangjifu@mail.sdu.edu.cn*
- *Meiqin Wang is with Quan Cheng Shandong Laboratory, Jinan, China. E-mail: mqwang@sdu.edu.cn*

*Manuscript received April **, ****; revised *****.*

dynamic window strategy. Our contributions are listed as follows.

TABLE 1
Summary of distinguishers on SIMON.

Block	Type	R	EDP/ELP	$\Delta_{in}/\Gamma_{in}^{\dagger}$	$\Delta_{out}/\Gamma_{out}^{\dagger}$	Ref.
48	Diff.	17	-46.32	$\{7\},\{1,5,9\}$	$\{1,5,9\},\{7\}$	[5]
		17	-46.38	$\{0\},\{2,18,22\}$	$\{2,18,22\},\{0\}$	[7]
		17	**-45.49**	$\emptyset,\{0\}$	$\{0\},\emptyset$	**Sect. 4**
	Linear	16	-44.92	$\{1,5,21\},\{23\}$	$\{1,5\},\{23\}$	[11]
		17	**-45.19**	$\{23\},\emptyset$	$\emptyset,\{23\}$	**Sect. 4**
64	Diff.	22	-61.32	$\{6,10\},\{7,11,12\}$	$\{6,10\},\{8\}$	[5]
		23	-61.93	$\{0\},\{2,30\}$	$\{2,6,30\},\{4\}$	[7]
		23	**-61.50**	$\{0,4\},\{6\}$	$\{6\},\{0,4\}$	**Sect. 4**
	Linear	21	-62.53	$\{20,24\},\{22\}$	$\{22\},\{20,24\}$	[12]
		23	**-60.24**	$\{25\},\{27,31\}$	$\{27,31\},\{25\}$	**Sect. 4**
96	Diff.	30	-92.2	$\{20\},\{6,14,18,22\}$	$\{8,16\},\{6,10,14\}$	[2]
		33	**-94.10**	$\emptyset,\{0\}$	$\{0\},\emptyset$	**Sect. 4**
	Linear	33	-92.60	$\{47\},\emptyset$	$\emptyset,\{47\}$	[9]
		33	**-91.74**	$\{47\},\emptyset$	$\emptyset,\{47\}$	**Sect. 4**
		34	**-93.74**	$\{47\},\emptyset$	$\{47\},\{45\}$	**Sect. 4**
128	Diff.	41	-123.74	$\{12\},\{6,10,14\}$	$\{6,10,14\},\{12\}$	[7]
		41	**-112.99**	$(\{6\},\{0,4,8\})$	$(\{0,4,8\},\{6\})$	**Sect. 4**
		41	**-122.98**	$(\emptyset,\{0\})$	$(\{0,6\},\emptyset)$	**Sect. 4**
	Linear	41	-123.07	$\{63\},\emptyset$	$\emptyset,\{63\}$	[9]
		43	**-124.59**	$\{63,59\},\{61\}$	$\emptyset,\{63,57\}$	**Sect. 4**

† The input and output differences (resp. masks) are denoted by $\{a_0,a_1,...,a_i\},\{b_0,b_1,...,b_j\}$ with a_i being the active position in the left branch while b_j denotes the active bits in the right branch. Note that $\emptyset$ means there is no active bit in this branch.

Dynamic Window (DW) with Minimal Loss. In Sect. 3, we show how to dynamically choose the window for each round based on two strategies: the MLW (Minimal Loss Window) strategy and the LWIM (Link Window in the Middle) strategy. The aim of MLW is to lose as few trails as possible, especially when the number of possibly activated bits is no bigger than the window size w. If the window size is run out, we will start to exclude some possibly active bits out of the window and restrict them as zero differences/masks. To maintain a lower loss of trails, those excluded bits are chosen using a reasonable probability test. With MLW, we can determine the windows in each round according to the propagation property from input difference/mask. Next, LWIM strategy will be used. For an $r(=2i+1)$-round cipher, windows in the first i rounds can be obtained with MLW using the input difference/mask. For the last i rounds, their windows are deduced by the output difference/mask from the decryption direction using MLW. Then, we heuristically link the windows in the middle round deduced from two directions to lose fewer trails. By using these approaches, we can get a DW that takes advantage of the diffusion property of the cipher. With SW, we perform several experiments on SIMON32 and find 9-bit DW can get a better result than the 13-bit SW shown in the upper part of Fig. 1, which means DW can get a tighter bound with less window size. We also use MLW and LWIM for SIMECK32 and show our result in the lower part of Fig. 1. DW for SIMECK32 is barely the same as the SW due to its slower diffusion. Hence, DW has the same effect compared to the SW for SIMECK32. To better compare DW with SW, we also apply these two methods to SIMON-like ciphers with different rotation constants. Eventually, we observe that DW can not only approach the lower bound of EDP or ELP faster than SW but is also suitable for variants with some special rotation constants $(c > a, b)$, where SW cannot deal with.

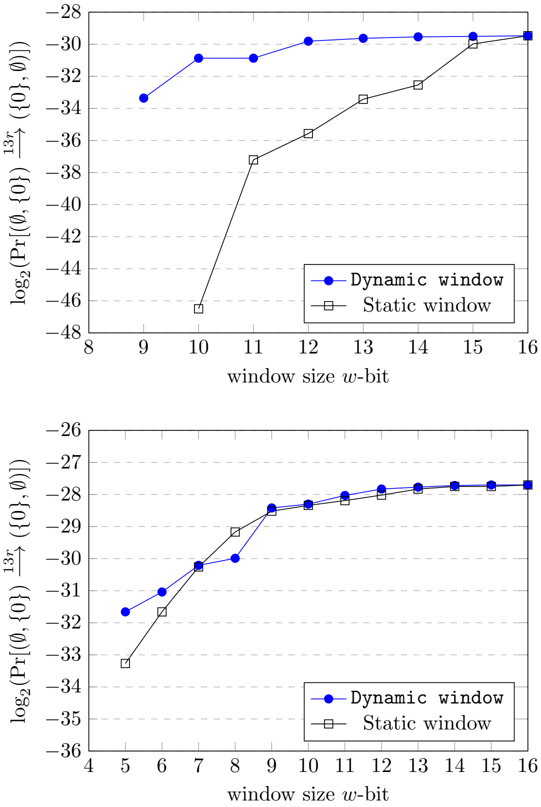

Fig. 1. Probability of a 13-round differential $(\emptyset,\{0\}) \rightarrow (\{0\},\emptyset)$ evaluated under different windows for SIMON32 (up) and SIMECK32 (down).

Improved Differential and Linear Hull. Our goal is to find the differential or linear hull suitable for key recovery attack. Thus, the lower hamming weight for the input and output differences/masks and the higher EDP/ELP for the distinguisher are our optimized objects. Using DW, we obtain a 17-round distinguisher for SIMON48 with a single active bit in the input and output for the first time, which can be used to mount more rounds of key-recovery attack. Moreover, the previous longest distinguisher for SIMON64 has 23 rounds and we improved the Hamming weight and probability for it. In addition, our identified 33-round distinguishers for SIMON96 have higher EDP/ELP compared to those from the static window strategy, which enables us to extend to 34-round distinguisher at the first time. Finally, we get the improved Hamming weight and the EDP for the previous best differential distinguisher for SIMON128. We compare our new distinguishers with the best previous ones in Table 1. Detailed results are illustrated in Sect. 4.

Improved Key Recovery Attacks on Round-Reduced SIMON. Based on our identified distinguishers, we perform differential key recovery attacks in Sect. 5 and linear key recovery attacks in Sect. 6 for SIMON, respectively. As exploited by Leurent *et al.* in [9], we adopt the dynamic-key guessing technique [13], [14] for differential cryptanalysis, and Fast Walsh Transform approach [15] for linear cryptanalysis. As a result, we provided the best differential/linear attacks on SIMON48, SIMON64, and SIMON96 in terms of the number

TABLE 2
Summary of attacks against SIMON.

Variant	Round	Attacked	Type	Data	Time	Succ. rate	Ref.
48/72	36	23	Diff.	2^{47}	$2^{63.25}$	0.48	[13]
		25		$\mathbf{2^{47}}$	$\mathbf{2^{67.89}}$	**0.42**	**Sect. 5**
		24	Linear	$2^{47.92}$	$2^{69.92}$	0.91	[4]
		26		$\mathbf{2^{47}}$	$\mathbf{2^{65.06}}$	**0.66**	**Sect. 6**
48/96	36	24	Diff.	2^{48}	$2^{78.99}$	0.48	[14]
		26		$\mathbf{2^{47}}$	$\mathbf{2^{92.51}}$	**0.42**	**Sect. 5**
		25	Linear	$2^{47.92}$	$2^{91.92}$	0.91	[4]
		27		$\mathbf{2^{47}}$	$\mathbf{2^{89.05}}$	**0.66**	**Sect. 6**
64/96	42	29	Diff.	2^{63}	$2^{86.94}$	0.48	[14]
		31		$\mathbf{2^{63}}$	$\mathbf{2^{91.43}}$	**0.41**	**Sect. 5**
		30	Linear	$2^{63.52}$	$2^{89.53}$	0.48	[4]
		32		$\mathbf{2^{63}}$	$\mathbf{2^{88.10}}$	**0.68**	**Sect. 6**
64/128	44	30	Diff.	2^{63}	$2^{110.99}$	0.48	[14]
		32		$\mathbf{2^{63}}$	$\mathbf{2^{123.89}}$	**0.41**	**Sect. 5**
		31	Linear	$2^{63.53}$	2^{120}	0.48	[4]
		33		$\mathbf{2^{63}}$	$\mathbf{2^{120.09}}$	**0.68**	**Sect. 6**
96/96	52	43	Linear	2^{94}	$2^{89.6}$	0.63	[9]
		44		$\mathbf{2^{95}}$	$\mathbf{2^{90.09}}$	**0.65**	**Sect. 6**
96/144	54	37	Diff.	2^{95}	$2^{132.25}$	0.46	[13]
		42		$\mathbf{2^{96}}$	$\mathbf{2^{140.53}}$	**0.56**	**Sect. 5**
		45	Linear	2^{95}	$2^{136.67}$	0.63	[9]
		45		$\mathbf{2^{95}}$	$\mathbf{2^{135.77}}$	**0.70**	**Sect. 6**
128/128	68	49	Diff.	2^{127}	2^{127}	0.73	[13]
		50		$\mathbf{2^{127}}$	$\mathbf{2^{127.07}}$	**0.60**	**Sect. 5**
		53	Linear	2^{127}	2^{121}	0.67	[9]†
		53		$\mathbf{2^{127}}$	$\mathbf{2^{120.72}}$	**0.67**	**Sect. 6**
128/192	69	49	Diff.	2^{127}	$2^{183.25}$	0.48	[13]
		51		$\mathbf{2^{127}}$	$\mathbf{2^{186.76}}$	**0.60**	**Sect. 5**
128/256	72	50	Diff.	2^{127}	$2^{247.25}$	0.48	[13]
		52		$\mathbf{2^{127}}$	$\mathbf{2^{250.76}}$	**0.60**	**Sect. 5**

† We recomputed the attack parameters using the distinguishers in [9] for better comparison.

of rounds, complexity, or success rate. We compare our key recovery attacks with the best previous ones in Table 2.

To allow our results to be reproduced, all source code utilized in this paper is available in an anonymous repository at https://github.com/Improved-Simon.

2 Some Known Properties and Analyses of SIMON

SIMONn/k [1] are Feistel ciphers with block size $n \in \{32, 48, 64, 96, 128\}$ and key size k. For each variant, their key size k and the number of rounds r are listed in Table 3.

TABLE 3
All variants of SIMON

n	32	48		64		96		128		
k	64	72	96	96	128	96	144	128	192	256
r	32	36	36	42	44	52	54	68	69	72

For the i-th round ($0 \leq i \leq r-1$), we respectively denote $x^{(i+1)}$ and $x^{(i)}$ as the left $n/2$-bit and right $n/2$-bit of the n-bit input state. Due to its Feistel structure, the right part of its output state is also $x^{(i+1)}$. The left output part is then denoted as $x^{(i+2)}$ and obtained with $x^{(i+2)} = x^{(i)} \oplus f\left(x^{(i+1)}\right) \oplus k^{(i)}$. The function f is a quadratic function designed to be $f(x) = (\mathrm{S}^8(x) \wedge \mathrm{S}^1(x)) \oplus \mathrm{S}^2(x)$, where $\mathrm{S}^a(x)$ denotes the a-bit left cyclic rotation of x, $\wedge$ as the bitwise AND, and $\oplus$ as the bit-wise exclusive or (XOR), respectively.

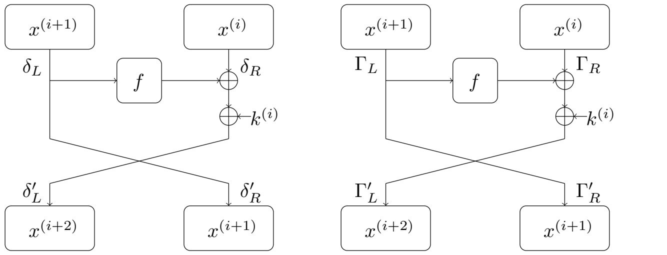

(a) Diff. $(\delta_L, \delta_R) \xrightarrow{f} (\delta'_L, \delta'_R)$. (b) Mask $(\Gamma_L, \Gamma_R) \xrightarrow{f} (\Gamma'_L, \Gamma'_R)$.

Fig. 2. Difference (left) and mask (right) propagation of one-round SIMON-like cipher.

The key schedule of SIMON is linear. Let $c = 2^{n/2} - 4 = \texttt{0xff}\cdots\texttt{fc}$ and z_j the constant sequence[1], the subkey of SIMON, with m key words $k^{(i+m)}$ are generated by:

$$\begin{cases} c \oplus (z_j)_i \oplus k^{(i)} \oplus \left(I \oplus S^{-1}\right) S^{-3} k^{(i+1)}, & \text{if } m = 2 \\ c \oplus (z_j)_i \oplus k^{(i)} \oplus \left(I \oplus S^{-1}\right) S^{-3} k^{(i+2)}, & \text{if } m = 3 \\ c \oplus (z_j)_i \oplus k^{(i)} \oplus \left(I \oplus S^{-1}\right) \left(S^{-3} k^{(i+3)} \oplus k^{(i+1)}\right), & \text{if } m = 4 \end{cases}$$

for $0 \leq i < r - m$, where $\mathrm{S}^{-a}(x)$ represents the a-bit right cyclic rotation of x. For more details of the constant sequence z_j, one can refer to [16].

Although SIMON uses a very simple quadratic round function, its differential and linear properties are hard to investigate due to the dependency between multiple active AND gates. In CRYPTO'15, Kölbl *et al.* constructed a systematic approach to deal with this dependency for SIMON-like round functions [5]. More precisely, they studied the differential and linear properties of functions of the form $f(x) = (\mathrm{S}^a(x) \wedge \mathrm{S}^b(x)) \oplus \mathrm{S}^c(x)$, where a, b and c are integer values. Here, we briefly recall their results.

Differential Cryptanalytic Property. As shown in Fig. 2a, we denote δ_L (resp. δ'_L) and δ_R (resp. δ'_R) as the input (resp. output) differences of the left and right parts, respectively. The propagation probability of one round $\Pr\left[(\delta_L, \delta_R) \to (\delta'_L, \delta'_R)\right]$ is

$$\begin{cases} 2^{-\dim\left(U_{\delta_L}\right)}, & \text{if } \delta_L = \delta'_R \text{ and } \delta_R \oplus \delta'_L \in U_{\delta_L} \\ 0, & \text{otherwise} \end{cases}$$

where U_{δ_L} is the coset of the image of a linear function $g(x)$ related to δ_L, *i.e.* $U_{\delta_L} = \mathrm{Img}(x \mapsto g(x) = f(x) \oplus f(x \oplus \delta_L) \oplus f(\delta_L) \oplus f(0))$, and $\dim(U_{\delta_L})$ represents its dimension. The probability of an r-round differential trail can then be evaluated by multiplying these probabilities of each round together. Thus, the probability of a differential can be obtained after summing the probabilities of all trails contained in this differential. However, there can be many trails and it's infeasible to consider all of them.

Linear Cryptanalytic Property. Input (resp. output) mask of the left and right parts are denoted as Γ_L (resp. Γ'_L) and Γ_R (resp. Γ'_R), as illustrated in Fig. 2b. The

[1] The constant sequence z_j uses as the round constants.

squared correlation of this one-round mask propagation $\mathrm{Cor}^2\left((\Gamma_L, \Gamma_R) \rightarrow (\Gamma'_L, \Gamma'_R)\right)$ is

$$\begin{cases} 2^{-\dim\left(V_{\Gamma_R}\right)}, & \text{if } \Gamma_R = \Gamma'_L \text{ and } \Gamma_L \oplus \Gamma'_R \in V_{\Gamma_R} \\ 0, & \text{otherwise} \end{cases}$$

where $V_{\Gamma_R} = \mathrm{Img}(x \mapsto ((\Gamma_R \wedge \mathsf{S}^{b-a}(x)) \oplus (\mathsf{S}^{-(b-a)}(\Gamma_R \wedge x))) \ggg a)$, and $x \ggg a$ denotes the a-bit right cyclic rotate of x. Squared correlation of the r-round linear trail can be obtained by multiplying these one-round squared correlations together. Summing all the squared correlations of trails comprising the linear hull, one can obtain its expected linear potential (ELP), as shown in [17]. However, this may also be infeasible.

Equivalence between Differential and Linear Trail. This is another important property of SIMON-like ciphers which has been observed by several works [18], [19], [20]. Specifically, given a differential trail with probability p, which is

$$(\delta_L^0, \delta_R^0) \rightarrow (\delta_L^1, \delta_R^1) \rightarrow \cdots \rightarrow (\delta_L^r, \delta_R^r),$$

a linear trail covering the same number of rounds written as

$$(\overleftarrow{\delta_R^0}, \overleftarrow{\delta_L^0}) \rightarrow (\overleftarrow{\delta_R^1}, \overleftarrow{\delta_L^1}) \rightarrow \cdots \rightarrow (\overleftarrow{\delta_R^r}, \overleftarrow{\delta_L^r})$$

with $\overleftarrow{x}$ being the bit-reversed x. However, the squared correlation of this linear trail may not equal to p [9] and shall be re-evaluated using the aforementioned method [5].

3 Dynamic Window for Transition Matrix

Given a differential or linear hull, it's hard to efficiently approximate its probability or ELP due to the massive number of trails contained in it. To deal with this, Leurent *et al.* [9] constructed an efficient framework for SIMON-like ciphers based on the difference transition matrix or linear correlation matrix M, which contains transition probability.

We recall their framework for evaluating the probability of a differential here. For each round, they built a square matrix M whose element in the i-th row and j-th column represents the propagation probability of the input difference δ_i and output difference δ_j. Those input and output differences are chosen heuristically. For matrices built for these middle rounds, the input differences are in the same set A and in the same order as the output differences. While for the first (resp. last) round, the output (resp. input) difference also belongs to this set A, but the input (resp. output) difference can be chosen heuristically. By multiplying all these matrices, they can obtain the total probability of the differential. In their approach, only trails whose active bits are located in a fixed w-bit window are considered in the matrix. The window is chosen to be those w least significant bits in each round. With this approach, they can gain longer differentials and linear hulls than before for both SIMON and SIMECK. For SIMON, they also found that there still exists a chance of potential improvement and encouraged further work on this cipher.

In this section, we follow the similar framework as Leurent *et al.* [9], however, a dynamic way to choose the w-bit window for each round is used. Firstly, we propose the MLW (short for minimal loss window) strategy and LWIM (short for link window in the middle) strategy to help us determine which bits shall be included in the window for each round in Sect. 3.1. Based on these dynamic windows, a modified algorithm for computing EDP or ELP is given at Sect. 3.2. We applied this modified framework on SIMON and SIMECK. Compared with the static windows adopted in [9], we can achieve better differentials and linear hulls for SIMON. Detailed application results are shown in Sect. 4.

3.1 New Strategies for Window Choosing

To make it clear, we introduce our strategies of choosing the window from the aspect of constructing the differential transition matrix for the differential.

For the linear hull, the equivalence between differential and linear trails described in Sect. 2 can be used to determine the window. Specifically, assuming we're dealing with the variant of block size n, we have to identify the w-bit window for the linear hull with input mask (δ_L^0, δ_R^0) and output mask (δ_L^r, δ_R^r). Note that for each trail in this linear hull, there is only one corresponding trail in the differential with input difference $(\overleftarrow{\delta_R^0}, \overleftarrow{\delta_L^0})$ and output difference $(\overleftarrow{\delta_R^r}, \overleftarrow{\delta_L^r})$, where $\overleftarrow{x}$ denotes the bit-reversed x. Hence, we can use our strategies to obtain the w-bit window chosen for this differential in each round. Assume that t_i^j with $0 \le i \le w-1$ comprises the window for the j-th round. Thus for the linear hull, the window chosen for the same round is composed of bits $\left((\frac{n}{2}-1) - t_i^j\right)$ where $0 \le i \le w-1$.

3.1.1 MLW: A Window with Minimal Loss.

By restricting the difference to the w-bit window, Leurent *et al.* construct a differential transition matrix that contains *all* trails only active at this window. In other words, they try to control the diffusion of the input difference by discarding all trails that diffuse out of the window. Windows in every involved rounds are chosen to be the w least significant bits. Due to the strong diffusion of non-linear part $w+5$ (for SIMECK) or $w+8$ (for SIMON) cyclic rotation, this strategy may lose many valuable trails even before the number of diffused bits exceed the window size, especially for SIMON. We show in Table 4 as an illustration where the input difference for SIMON48 is set to be $(\emptyset, \{0\})$ and the window size is 17. Note that the static window chosen by Leurent *et al.* is in the range between 0 and 16. Hence, the 17-th and 18-th bits in the fourth round are discarded. However, we run out of the window only after the fifth round. Thus, it will be better if we only discard trails after running out of the window size.

In our MLW strategy, we keep all trails before the window size is running out. When the number of diffused bits exceeds the window size, we discard some bits with the aim of losing less trails according to the Minimal Active Probability Test.

Minimal Active Probability Test (Considering Dependency). Assume that the input difference of the differential is $\triangle_{in}$. We respectively denote $\mathcal{B}^{(j)}$ and $\mathcal{D}^{(j)}$ as the number of diffused bits and discarded bits in the j-th round. Therefore, we have $\binom{\mathcal{B}^{(j)}}{\mathcal{D}^{(j)}}$ cases of the possible discarded bits. In the following, we focus on how to determine the window in the j-th round. Whatsmore, we only need to determine the window of the left part of the j-round output state because the right window is the same as the window of the left part of the input state.

TABLE 4
Comparison of the bit loss on SIMON48 with different 17-bit window, where bits bolded are discarded by our dynamic window. Note that the static window is composed of bits 0, 1, · · · , 16.

Round	Diffusion bit position with input difference $(\emptyset, \{0\})$	Dynamic	Static [9]
0	[]	0	0
1	[0]	0	0
2	[1,2,8]	0	0
3	[0,2,3,4,9,10,16]	0	0
4	[0,1,3,4,5,6,8,10,11,12,17,18]	0	2
5	[0,**1**,2,3,4,5,6,7,8,9,10,**11**,12,13,14,16,18,19,20]	2	3
6	[**0**,1,2,3,4,5,**6**,**7**,8,9,10,11,12,**13**,14,15,16,17,18,**19**,**20**,21,22]	6	6
7(full)	[0,**1**,2,3,**4**,**5**,6,7,8,9,10,11,12,13,14,**15**,16,17,18,**19**,20,**21**,**22**,23]	7	7
8	[**0**,1,2,**3**,4,5,**6**,**7**,8,9,**10**,11,12,13,14,15,16,**17**,18,19,20,21,22,**23**]	7	7

To get a window with minimal loss of trails, we consider the probability $\Pr_c$ of the number of kept trails among all possible trails in the differential covering the previous j rounds. Note that $\Pr_c$ is equal to the probability of a truncated differential with a fixed input difference $\triangle_{in}$, while the output difference is a truncated difference $\triangle^{\star}_{out}$. This truncated difference $\triangle^{\star}_{out}$ has zero differences on these $\mathcal{D}^{(i)}$ bits while other bits can be active or not. Note that $\triangle^{\star}_{out}$ takes all zero differences on bits that will never be diffused. The probability $\Pr_c$ can be reasonably estimated as follows. We randomly construct N plaintext pairs satisfying the input difference $\triangle_{in}$, and then calculate how many pairs fulfilling the truncated difference $\triangle^{\star}_{out}$. Then, we formally define the estimate of $\Pr_c$ as

$$\Pr_c \approx \frac{1}{N}\#\{x \in \{0,1\}^n : \mathrm{E}(x) \oplus \mathrm{E}(x \oplus \triangle_{in}) = \triangle^{\star}_{out}\}.$$

For each case of those $\mathcal{D}^{(i)}$ possible discarded bits, we can obtain its corresponding $\Pr_c$, and then choose the case that with the maximal $\Pr_c$ to discard these $\mathcal{D}^{(i)}$ bits.

Take SIMON48 for an example. When the input difference is $(\emptyset, \{0\})$, the diffused bits in each round is shown in Table 4. As one can see, we run out the window size 17 at the fifth round. Hence, we need to determine which bits to be discarded from the 19 bits, which leads to $\binom{19}{2} = 171$ cases. Similarly, there are $\binom{23}{6} \approx 2^{16.62}, \binom{24}{7} \approx 2^{18.4}$ and $\binom{24}{7} \approx 2^{18.4}$ cases for the 6-th, 7-th and 8-th round, respectively. For each case, we obtain its $\Pr_c$ utilizing $N = 2^{24}$ plaintext pairs. To gain an accurate estimation, N is chosen to be 2^{24} here since it can ensure that the estimated value of $\Pr_c$ is stable. As a result, those bits bolded in Table 4 are discarded. Compared with the static window, our dynamic window have the less chance of losing trails.

However, for the variant with larger state, the above test cannot be proceeded since the number of cases for discarded bits are unpractical for us to compute. More precisely, for SIMON64, the cases of discarded bits reach $\binom{20}{3} \approx 2^{10.15}, \binom{26}{9} \approx 2^{21.58}, \binom{30}{13} \approx 2^{26.84}$ and $\binom{32}{15} \approx 2^{29.08}$ at 5-th, 6-th, 7-th, and 8-th round, respectively. Even if $N = 2^{24}$, we need to test $2^{24} \times \binom{20}{3} \approx 2^{34.15}, 2^{24} \times \binom{26}{9} \approx 2^{45.58}, 2^{24} \times \binom{30}{13} \approx 2^{50.15}, 2^{24} \times \binom{32}{15} \approx 2^{53.08}$ for 5-th, 6-th, 7-th, and 8-th round, respectively.

Minimal Active Probability Test (Independent). Due to the unsolvable cases of discarded bits, we can not obtain the window for variants with a large state. To deal with this, we assume that each bit in the same round is independent with the others and then test the probability of single bit being active using lots of plaintext pairs fulfilling the fixed input difference $\triangle_{in}$. In this case, we will discard $\mathcal{D}^{(i)}$ bits that have the lowest probability. We implemented this test on SIMON48 with the same input difference $(\emptyset, \{0\})$, and observed that the 17-bit window deduced from this test is the same as that illustrated in Table 4. This implies that the assumed independence can be satisfied here. However, as the number of test rounds grows, the probability of each bit being active will be close to 1/2, which means the test can only work around the full diffusion round.

3.1.2 LWIM: A Combined Window Location Strategy.

As one can see from the above MLW strategy, we only care about the diffusion from the input difference $\triangle_{in}$, while the output difference $\triangle_{out}$ of the differential is not considered. However, the above one-way strategy cannot ensure all trails satisfy $\triangle_{out}$. Hence, we propose the LWIM (link window in the middle) strategy here locating the MLW in forward and backward directions to contain as many trails as we can.

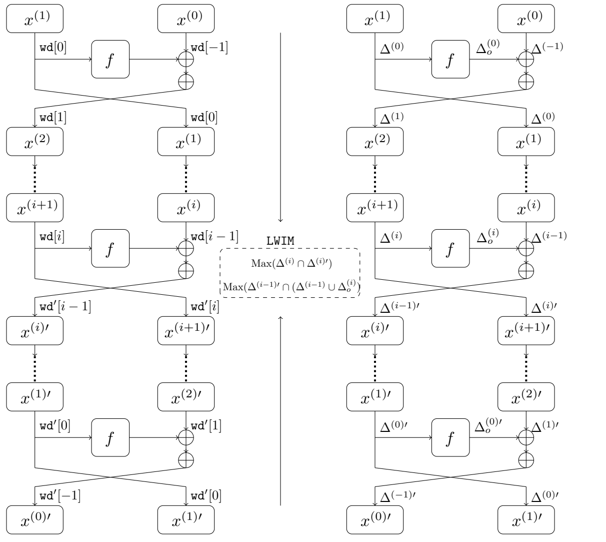

Fig. 3. LWIM strategy. $\Delta^{(j)}$ (resp. $\Delta^{(j)'}$) is the set containing all differences where only bits in the window wd[j] (resp. wd′[j]) can take non-zero differences.

As shown in Fig. 3, assuming that we are targeting at an r-round cipher with $r = 2i + 1$, we need to determine the dynamic windows for the differential $(\delta_L^{(0)}, \delta_R^{(0)}) \rightarrow (\delta_L^{(0)'}, \delta_R^{(0)'})$. With the MLW strategy, one can obtain the windows wd[j] for the first i rounds according to the diffusion of its input difference. Meanwhile, dynamic windows wd$'$[j] in the last i rounds can also be deduced from its output difference using the MLW strategy.

However, for the middle round, we have to check whether the windows wd[$i+1$], wd[i], wd$'$[$i+1$] and wd$'$[i] which are respectively chosen for the states $x^{(i+1)}$, $x^{(i)}$, $x^{(i)'}$ and $x^{(i+1)'}$ can be used together. We denote $\Delta^{(j)}$ (resp. $\Delta^{(j)'}$) as the set containing all possible differences that only takes non-zero differences on bits in the window wd[j] (resp. wd$'$[j]). Meanwhile, we use $\Delta_0^{(i)}$ to represent the set composed of all output differences of f in the middle round.

In order not to lose too much trails in the middle round, we have to maximize the size of $\Delta^{(i)} \cap \Delta^{(i)'}$ and $\Delta^{(i-1)'} \cap (\Delta^{(i-1)} \cup \Delta_0^{(i)})$, where the symbol $\cap$ and $\cup$ respectively denote the intersection and union between two sets. The sizes of these two sets are actually determined by the input and output differences of the target differential. A trivial way to maximize their size is to restrict the differential as $\delta_L^{(0)} = \delta_R^{(0)'}$ and $\delta_R^{(0)} = \delta_L^{(0)'}$. In this case, the dynamic windows wd[j] will be the same as wd$'$[j], as well as the difference sets $\Delta^{(j)}$ and $\Delta^{(j)'}$. Hence, we can obtain that $\Delta^{(i)} \cap \Delta^{(i)'} = \Delta^{(i)}$ and $\Delta^{(i-1)'} \cap (\Delta^{(i-1)} \cup \Delta_0^{i}) = \Delta^{(i-1)}$, which can save as many trails as we can to a certain extent.

3.2 Modified Algorithm for Computing Transition Probability

Recall that when using the static windows, the difference sets $\Delta^{(j)}$ and $\Delta^{(j)'}$ are equal for all rounds j. In other words, with the notation used in Fig. 3,

$$\Delta^{(-1)} = \Delta^{(0)} = \cdots = \Delta^{(i)} = \cdots = \Delta^{(0)'} = \Delta^{(-1)'}.$$

Therefore, the differential propagation matrix (resp. linear transition matrix) in each round are indexed with the same difference (resp. mask) values. However, when dynamically choosing the window for each round, the matrices will have different indexes since the difference sets in each round are different. Note that in our dynamic window strategy, we only restrict that $\Delta^{(j)} = \Delta^{(j)'}$ while no restrictions on these $\Delta^{(j)}$ or $\Delta^{(j)'}$ in each round are applied. To deal with these different indexes, we established a hash table to store the index of each matrix.

Next, we will detail our modified algorithm that evaluates EDP for a differential as follows and focus on the one-round propagation. We denote $\delta_L^{(i)}$ ($\delta_R^{(i)}$) and $\Delta_L^{(i)}$ ($\Delta_R^{(i)}$) as the input differences and its set of the left (right) branch of the i-th round, respectively. At first, we generate all possible $\delta_L^{(i)}$ and $\delta_R^{(i)}$ according to the corresponding w-bit dynamic windows. Specifically, they can only have non-zero differences on bits contained in the window. Secondly, we compute the output difference γ of the f function and check whether $\gamma \in U_{\delta_L^{(i)}}$. If so, we can obtain $\delta_L^{(i+1)}$ and then check whether keep it according to its window. Similar as [9, Algorithm 1], the complexity of the algorithm is bounded by $r \times 2^{2w} \times \max_{\delta_L^{(i)} \in \Delta_L^{(i)}} |U_{\delta_L^{(i)}}|$ elementary operations. We assume that the time complexity of the hash lookup table is negligible compared to floating-point arithmetic. With the help of hash tables, we can efficiently update the differential propagation matrix indexed by $(\delta_R^{(i)} \oplus \gamma, \delta_L^{(i)})$ and finally obtain EDP of the differential. Details of the above procedure have been described in Algorithm 1.

Algorithm 1 Computation of Probability Using Transition Matrix

```
Input: An $r$-round differential $(\delta_L^{(0)}, \delta_R^{(0)}) \rightarrow (\delta_L^{(r)}, \delta_R^{(r)})$
    with its dynamic windows.
Output: EDP of the differential.

$X \leftarrow [0$ for $i \in \Delta_L^{(0)},\ j \in \Delta_R^{(0)}]$
$X[\delta_L^{(0)}, \delta_R^{(0)}] \leftarrow 1$
for $1 \le i < r$ do
    set $\Delta_L^{(i)} \leftarrow \delta_L^{(i)}$ restricted by window;
    set $\Delta_R^{(i)} \leftarrow \delta_R^{(i)}$ restricted by window;
    for each $\delta_L^{(i)} \in \Delta_L^{(i)}$ do
        for each $\delta_R^{(i)} \in \Delta_R^{(i)}$ do
            for each $\gamma \in U_{\delta_L^{(i)}}$ do
                if $(\delta_R^{(i)} \oplus \gamma)$ fulfills its window then
                    $Y[\delta_R^{(i)} \oplus \gamma, \delta_L^{(i)}] \leftarrow$
                    $Y[\delta_R^{(i)} \oplus \gamma, \delta_L^{(i)}] + 2^{\text{-dim}(U_{\delta_L^{(i)}})} X[\delta_L^{(i)}, \delta_R^{(i)}]$
                end if
            end for
        end for
    end for
    $X \leftarrow Y$
end for
return $X[\delta_L^{(r)}, \delta_R^{(r)}]$
```

4 Application of the Dynamic Window Strategy

We applied the dynamic window strategy on evaluating EDP and ELP for almost all variants of SIMON and obtained better distinguishers. The largest window size we can choose is 17-bit, which consumes 256GB of memory size. All of our distinguishers were evaluated using a 17-bit dynamic window. We also note that all the tests in this section are implemented on a server with AMD EPYC 7302 16-Core Processor, and the RAM size is 256GB.

A Heuristic Setting Method for DW *to Reach a Local Optimal.* As explained in Sect. 3, DW tracks all diffused bits for the given difference. Besides, DW will not discard trails when the number of diffused bits is less than the window size. However, SW starts discarding tails even though there is still room for them. Thus, DW can keep less loss of trails and take more advantage of the diffusion property of the cipher. To determine the MLW, we use a minimal active probability test, which can detect the bits with a low probability of being active in the first few rounds. However, as the number of rounds grows, the probability of each bit being active will be close to 1/2. Meanwhile, the minimal active probability test cannot suggest clearly which bits should be excluded in this case. Thus, to promise accuracy, MLW can only be used to determine windows until we are around the full diffusion round. Let's take SIMON as an example. Since the full diffusion of SIMON occurs near eight rounds, we can obtain the exact 8-round DW using MLW. Next, we use two 8-round DW using MLW (generated from forward and backward directions) and link them using LWIM in the middle (one additional linking round is needed). In this case, we can obtain a local optimal 17-round DW for differential $(\emptyset, \{0\}) \to (\{0\}, \emptyset)$.

Application on SIMON48. With the MLW and LWIM strategies, we divided the cipher into two parts, and obtained the local optimal 17-bit DW for a 17-round differential $(\emptyset, \{0\}) \to (\{0\}, \emptyset)$. We show the DW in Appendix. The input and output differences are denoted by $(\{a_0, a_1, \cdots\}, \{b_0, b_1, \cdots\})$ with a_i being the active position in the left branch while b_j denotes the active bits in the right branch. Note that $\emptyset$ means there is no active bit in this branch. The 17-round differential has the probability of $2^{-45.49}$. Meanwhile, we obtained the ELP of the 17-round linear hull $(\{23\}, \emptyset) \to (\emptyset, \{23\})$ whose DW can be determined due to the duality between differential and linear trails, as explained in Sect. 3.1. The ELP of this linear hull is $2^{-45.19}$. We also compare DW with the SW in Fig. 4.

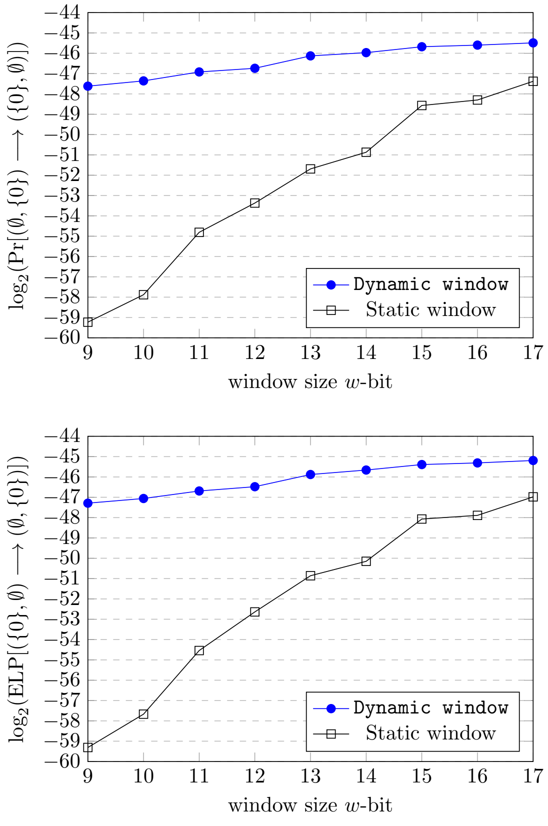

Fig. 4. EDP (left) and ELP (right) of the 17-round differential and linear hull for SIMON48.

Construct the DW for longer differentials from the Local Optimal 17-Round One. As aforementioned, the 17-round DW for the differential $(\emptyset, \{0\}) \to (\{0\}, \emptyset)$ is a local optimal one with single active bit of input-output difference for SIMON. To obtain DW for differentials covering more rounds (> 17) and fully utilize this local optimal differential, we adopt two approaches. Firstly, one can append an optimal trail covering a short number of rounds before and after the 17-round one. In this case, a differential with multi-active bits of input-output difference can be obtained. Note that DW in these added top and bottom rounds can also be determined with MLW. Given this DW, EDP of this multi-active bits differential can be evaluated using Algorithm 1. Hence, DW discovers an effective multi-active bits differential covering more than 17 rounds. This is also one of the advantages of DW. The second approach utilizes the 17-round local optimal differential $(\emptyset, \{0\}) \to (\{0\}, \emptyset)$, as well as the differential $(\emptyset, \{0\}) \to (\emptyset, \{0\})$ covering its top 16 rounds and the differential $(\{0\}, \emptyset) \to (\{0\}, \emptyset)$ covering its bottom 16 rounds. EDPs of these two 16-round differentials are the same as that of the 17-round one. Thus, one can construct a longer differential by cascading these two or three differentials. EDP of this longer differential can be computed with Algorithm 1, where its DW can be constructed with DW for these three differentials.

Application on SIMON64. Based on the 17-round differential, we follow the first approach where three rounds are respectively added before and after it to construct 23-round multi-active bits differential $(\{0, 4\}, \{6\}) \to (\{6\}, \{0, 4\})$ for SIMON64. The DW for this 23-round differential is shown in Appendix. With Algorithm 1, its EDP is $2^{-61.50}$. Similarly, using the DW for the differential and the duality of linear trails, we obtained the 23-round $(\{25\}, \{27, 31\}) \xrightarrow{23r} (\{27, 31\}, \{25\})$ linear hull with ELP $2^{-60.24}$. For comparison, we also use a 17-bit SW to re-evaluate the EDP and ELP of these newly discovered distinguishers. As a result, EDP of the 23-round differential is $2^{-62.88}$, while the ELP for the linear hull is $2^{-61.36}$. Both are worse than those evaluated under 17-bit DW.

Application on SIMON96. We constructed a 33-round differential $(\emptyset, \{0\}) \xrightarrow{33r} (\{0\}, \emptyset)$ following the second approach, which is the same differential proposed by [9]. However, with our Algorithm 1, this differential can have a higher EDP than theirs due to the local optimal DW. More precisely, its EDP is $2^{-94.10}$. The distinguisher is constructed as $(\emptyset, \{0\}) \xrightarrow{16r} (\emptyset, \{0\}) \xrightarrow{1r} (\{0\}, \emptyset) \xrightarrow{16r} (\{0\}, \emptyset)$. We show the DW in Appendix. Meanwhile, we can obtain a linear hull $(\{47\}, \emptyset) \xrightarrow{33r} (\emptyset, \{47\})$ with ELP $2^{-91.74}$. Similar to [9], we can append one round after the distinguisher with the loss of ELP 2^{-2}. Hence, a 34-round linear hull $(\{47\}, \emptyset) \xrightarrow{34r} (\{47\}, \{45\})$ can be achieved with ELP $2^{-93.74}$.

Application on SIMON128. For SIMON128, we utilized a 33-round local optimal DW and appended eight rounds of SW after the 33-round DW to construct a 41-round one. Finally, we obtained a 41-round differential $(\emptyset, \{0\}) \xrightarrow{41r} (\{0, 6\}, \emptyset)$ with EDP of $2^{-122.98}$. Then, with the 41-round DW, we obtained a linear hull $(\{63\}, \emptyset) \xrightarrow{41r} (\emptyset, \{57, 63\})$ with ELP $2^{-120.59}$. Similarly, we append two rounds on the top of the linear hull with the loss of ELP 2^{-4} to get a 43-round one whose input mask is $(\{63, 59\}, \{61\})$.

5 Key-Recovery Attacks Using Differential Cryptanalysis

In this section, we detail differential key-recovery attacks against SIMON using dynamic key-guessing technique [13], [14]. We denote the involved key as k_p, k_f on the plaintext side, and k_b, k_c on the ciphertext side (shown in Fig. 5), and the number of the key bits as κ_p, κ_f (κ_b, κ_c). The total number of the involved key bits is denoted as $\kappa_g = \kappa_p + \kappa_f +$

$\kappa_b + \kappa_c$. Then, we briefly recall this technique and introduce our attacks in Sect. 5.2.

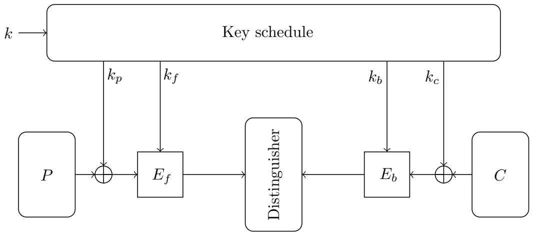

Fig. 5. General description of a cipher.

5.1 Dynamic Key-Guessing Technique [8], [14]

The main idea of dynamic key-guessing is to remove the redundancy of the guessed subkey according to the immediate values of a given differential path, and the process of the attack is as follows.

Sufficient Conditions. Based on the R-round distinguisher $\Delta_i \to \Delta_o$, we append r_f rounds before and r_b rounds after and build the extended differential for our key recovery attacks. Then we can identify the sufficient bit conditions as shown in Table 5.

Data Collection. First, we build structures of plaintexts where the bits with a fixed difference in round one are identical for all the plaintexts in S_1 and S_2, where S_1 and S_2 denote two structures with fixed differences. Each structure is composed of 2^{n-l_1} plaintexts, where l_1 denote the number of the fixed bits at round one. For each structure, we encrypt the plaintexts and obtain the corresponding ciphertexts, totally $D \times 2^{n-l_1}$ encryption, where D denotes the data complexity. Then, we can pair these ciphertexts and filter them at the output according to the fixed difference in C, and $2^{2(n-l_1)-l_{r-1}}$ pairs remain in each pair of structure.

Key Recovery. Then, we need to associate partial key guesses to each of these pairs and make sure they can validate the difference of distinguisher. From the outer to the inner, for each sufficient bit condition, we associate to each pair the possible combinations of key bits that lead to the desired input-output difference of the distinguisher. For each pair, we increment the corresponding counters of the combination of key bits that lead to Δ_i and Δ_o. In total, we have incremented $\lambda_W \times 2^{\kappa_g}$ counters on average, with λ_W the average value of a counter for a wrong key guess. After processing all pairs, we set a threshold s, and for each counter greater than s, we store them as the key candidate. Finally, we exhaustively search the remaining key bits not guessed under these key candidates and construct the master key.

Complexity and Success Probability. We denote the average value of counters for the right key λ_R for the wrong key λ_W, and then we estimate them for computing the complexity and the success probability. For each plaintext P_1 in S_1 and for each key guess, we compute $P_2 = E_f^{-1}(E_f(P_1 \oplus \Delta_i))$ such that $E_f(P_1) \oplus E_f(P_2) = \Delta_i$. So, for each key guess, two plaintexts form a pair, and we have $D/2$ pairs with the desired difference at the input of our distinguisher. For the right key guess, if the distinguisher probability is p, we have $\lambda_R = p \times D/2$ pairs that satisfy Δ_o. By construction, all these pairs belong to the structures and pass the filters. For the wrong key guesses, the probability that they have a fixed difference Δ_o at the output is $1/2^n$, and the counter is expected to be $\lambda_W = D/2^{n+1}$ on average.

Similar to [9], [13], [14], we apply the Poisson distribution as the statistical model and denote the corresponding cumulative distribution function as F_W and F_R. The probability that a counter associated with the wrong key guess is greater than threshold s is $1 - F_W(s)$, and the expected number of counters greater than s is $2^{\kappa_g}(1 - F_W(s))$. Due to the linear key schedule of SIMON, we can reconstruct the master key candidates from any subkey bits using linear algebra. The cost of reconstructing the master keys is $2^{\kappa_g} \cdot (1 - F_W(s)) \times 2^{\kappa - \kappa_g} = 2^{\kappa} \cdot (1 - F_W(s))$. The time complexity and success probability are:

$$C_1 = D + 2^{\kappa_g} \cdot \lambda_W + 2^{\kappa} \cdot (1 - F_W(s))$$
$$P_S = 1 - F_R(s)$$

5.2 25-Round Key-Recovery on SIMON48/72

We apply the method with the differential $(\emptyset, \{0\})$ to $(\{0\}, \emptyset)$ covering 17 rounds with probability $p = 2^{-45.49}$, and append three rounds before and five rounds after it. We show the detail of the bits to guess round by round in Table 6. From the outer to the inner, we use the sufficient bit conditions from Table 5 to guess the key bits that lead to the desired differences. When possible, we use the guessed key bits to deduce other key bits using the key schedule. In the rightmost column, we detail the time complexity of each step starting from 2^t pairs. In total, the complexity of guessing the key bits leading to Δ_i and Δ_o, and incrementing the corresponding counters is 2^{t+32}. During this step, $\kappa_g = 69$ bits, from the first subkeys to the last subkeys are guessed.

Attack Parameters. If the data $D = 2^{47}$ is taken, knowing that $l_1 = 41$ and $l_{24} = 18$, we split the data into 2^{40} structures of 2^7 plaintexts and after constructing our pairs of structures and filtering the ciphertexts C, there remain $2^{40-1} \times 2^{7\times 2}/2^{18} = 2^{35}$ pairs. So $t = 35$ and the time complexity for the counter incrementing part is $2^{t+32} = 2^{67}$. The average value for the counter of the right key guess is $\lambda_R = p \times D/2 = 2^{0.51}$. For a bad key guess, we expect the counter to be close to $\lambda_W = D/2^{48+1} = 2^{-2}$. We choose the subkeys whose counts are greater than 1, the complexity is $2^{67} + 2^{66.76} \approx 2^{67.89}$ with a success probability of 42%.

We show parameters for different variants of SIMON in Table 7.

6 Key-Recovery Attacks Using Linear Cryptanalysis

In this section, we detail our key recovery attack using linear cryptanalysis. We follow the description of a last-round key recovery given by Matsui's Algorithm 2 [21] and consider a linear approximation $P' \cdot \alpha \oplus C' \cdot \beta$ where P' and C' the intermediate values after a few rounds of encryption/decryption. Given a set of D known plaintext/ciphertext pairs (P, C), we can compute the intermediate values P' and C' for each partial key guess $\kappa_g =$

TABLE 5
Extended path for 25 rounds of SIMON48/72, where bold bits represent the sufficient bit conditions.

r	Differential path		l_i
0	0000000⋆00000⋆⋆00001⋆⋆01	00000⋆⋆0000⋆⋆⋆0⋆01⋆⋆⋆0⋆⋆	32
1	000000000000000⋆000001⋆0	0000000⋆00000⋆⋆00001⋆⋆01	41
2	0000000**0**00000**00**00000**00**01	000000000000000⋆000001⋆0	46
3	000000000000000**0**000000**0**0	000000000000000000000001	48
	17-round differential ($3 \to 20$)		
20	000000000000000000000001	000000000000000**0**000000**0**0	48
21	000000000000000⋆000001⋆0	0000000**0**00000**00**00000**00**01	46
22	0000000⋆00000⋆⋆00001⋆⋆01	00000**00**0000**000**0⋆00**000**1⋆**0**	41
23	00000⋆⋆0000⋆⋆⋆0⋆01⋆⋆⋆0⋆⋆	000**000**0⋆0**0000**⋆⋆**00001**⋆⋆**01**	32
24	000⋆⋆⋆0⋆0⋆⋆⋆⋆⋆⋆⋆⋆⋆⋆⋆⋆⋆⋆⋆	00000⋆⋆0000⋆⋆⋆0⋆01⋆⋆⋆0⋆⋆	18
25	0⋆⋆⋆⋆⋆⋆⋆⋆⋆⋆⋆⋆⋆⋆⋆⋆⋆⋆⋆⋆⋆⋆⋆	000⋆⋆⋆0⋆0⋆⋆⋆⋆⋆⋆⋆⋆⋆⋆⋆⋆⋆⋆⋆	6

TABLE 6
Details of the bits to guess round by round and the corresponding complexity when starting from 2^t pairs.

R	Bits to guess	total	#cond.	Complexity
23	$k^{(24)}_{0,3,4,5,6,7,10,11,12,13,16,17,18,19,20,21,22,23}$.	18	14	$2^t \cdot 2^{18-14} = 2^{t+4}$
22	$k^{(23)}_{2,3,4,9,10,11,16,17,19,20,21,23}$, $k^{(24)}_{1,2,8,9,15}$	17	9	$2^{t+4} \cdot 2^{17-9} = 2^{t+12}$
21	$k^{(24)}_{14}$, $k^{(23)}_{0,1,6,7,8,13,14,18}$, $k^{(22)}_{1,8,9,15,18,19}$	15	5	$2^{t+12} \cdot 2^{15-5} = 2^{t+22}$
20	$k^{(23)}_{5,15,22}$, $k^{(22)}_{5,6,16,23}$, deduced $k^{(21)}_{7,17}$	7	2	$2^{t+22} \cdot 2^{7-2} = 2^{t+27}$
2	$k^{(0)}_{1,8,9,15,18,19}$	6	5	$2^{t+27} \cdot 2^{6-5} = 2^{t+28}$
3	$k^{(0)}_{5,6,16,23}$, $k^{(1)}_{7,17}$	6	2	$2^{t+28} \cdot 2^{6-2} = 2^{t+32}$

TABLE 7
Attack parameters for differential attacks on SIMON. We denote the success probability as P_S, and all the attacks used the distinguishers in Table 1. We set the threshold $s = 1$.

Variant	Rounds	κ_g	D	λ_R	λ_W	P_S	Time
48/72	25=3+17+5	69	$2^{47.5}$	$2^{1.01}$	$2^{-1.5}$	0.60	$2^{68.58}$
48/72	25=3+17+5	69	2^{47}	$2^{0.51}$	2^{-2}	0.42	$2^{67.89}$
48/96	26=4+17+5	94	$2^{47.5}$	$2^{1.01}$	$2^{-1.5}$	0.60	$2^{93.14}$
48/96	26=4+17+5	94	2^{47}	$2^{0.51}$	2^{-2}	0.42	$2^{92.51}$
64/96	31=4+23+4	92	$2^{63.5}$	2^{1}	$2^{-1.5}$	0.59	$2^{92.20}$
64/96	31=4+23+4	92	2^{63}	$2^{0.5}$	2^{-2}	0.41	$2^{91.43}$
64/128	32=4+23+5	124	$2^{63.5}$	2^{1}	$2^{-1.5}$	0.59	$2^{124.58}$
64/128	32=4+23+5	124	2^{63}	$2^{0.5}$	2^{-2}	0.41	$2^{123.89}$
96/144	42=4+33+5	124	2^{96}	$2^{0.9}$	2^{-1}	0.56	$2^{140.53}$
128/128	50=4+42+4	105	2^{127}	$2^{1.02}$	2^{-2}	0.60	$2^{127.07}$
128/192	51=5+42+4	159	$2^{127.5}$	$2^{1.52}$	$2^{-1.5}$	0.78	$2^{187.67}$
128/192	51=5+42+4	159	2^{127}	$2^{1.02}$	2^{-2}	0.60	$2^{186.76}$
128/256	52=5+42+5	208	2^{127}	$2^{1.02}$	2^{-2}	0.60	$2^{250.76}$

$(\kappa_p, \kappa_f, \kappa_b, \kappa_c)$ for the first and/or last rounds, and compute the experimental correlation of the linear approximation

$$\begin{aligned} q\left(k_p, k_f, k_b, k_c\right) &= \frac{1}{D}(\#\left\{P, C : P' \cdot \alpha \oplus C' \cdot \beta = 0\right\} \\ &\quad - \#\left\{P, C : P' \cdot \alpha \oplus C' \cdot \beta = 1\right\}) \\ &= \frac{1}{D}\sum_{P,C}(-1)^{P' \cdot \alpha \oplus C' \cdot \beta} \end{aligned}$$

The value of $P' \cdot \alpha$ and $C' \cdot \beta$ is computed as a function of the partial key guess and some bits in plaintext and ciphertext, and we denote the masked bits as $\chi_p(P)$ and $\chi_c(C)$. Then, we have:

$$\begin{aligned} P' \cdot \alpha &= f\left(k_f, k_p \oplus \chi_p(P)\right) \\ C' \cdot \beta &= g\left(k_b, k_c \oplus \chi_c(C)\right) \end{aligned}$$

6.1 FWT Approach [22], [23]

Since the value of $P' \cdot \alpha$ and $C' \cdot \beta$ do not depend on the full plaintext/ciphertext, we can compress the dataset using a distillation phase [21] where we only count the number of plaintext/ciphertext pairs that reach each value of P' and C', then we correlate $q\left(k_p, k_f, k_b, k_c\right)$

$$\begin{aligned} &= \frac{1}{D}\sum_{P,C}(-1)^{f(k_f, k_p \oplus \chi_p(P)) \oplus g(k_b, k_c \oplus \chi_c(C))} \\ &= \frac{1}{D}\sum_{i \in \mathbb{F}_2^{\kappa_p}}\sum_{j \in \mathbb{F}_2^{\kappa_c}} \#\left\{P, C : \chi_p(P) = i, \chi_c(C) = j\right\} \\ &\times (-1)^{f(k_f, k_p \oplus i) \oplus g(k_b, k_c \oplus j)} \end{aligned}$$

where i and j denote the masked value of plaintext and ciphertext. Then, we can find that the expression above is a convolution:

$$\begin{aligned} &\frac{1}{D}\sum_{i,j}\phi(i, j) \times \psi_{k_f, k_b}\left(k_p \oplus i, k_c \oplus j\right) \\ &= \frac{1}{D}\left(\phi * \psi_{k_f, k_b}\right)\left(k_p, k_c\right) \end{aligned}$$

where

$$\begin{aligned} \phi(x, y) &= \#\left\{P, C : \chi_p(P) = x, \chi_c(C) = y\right\} \\ \psi_{k_f, k_b}(x, y) &= (-1)^{f(k_f, x) \oplus g(k_b, y)} \end{aligned}$$

Therefore, for a given k_f, k_b, we can evaluate $q(k_p, k_f, k_b, k_c)$ for all k_p, k_c with complexity $\tilde{\mathcal{O}}(2^{\kappa_p + \kappa_c})$ using a Fast Walsh Transform, which is first observed in [22], and then generalized in [23]. The time complexity of the analysis phase is reduced to $\tilde{\mathcal{O}}(D + 2^{\kappa_g})$.

6.2 Statistical Models to Estimate Success Probability

We follow the work of Blondeau and Nyberg [24], [25] to estimate the success probability of the attack. Similarly, the sampling model with a factor B depends on the type of attack: $B = 1$ if the plaintexts are randomly chosen with repetition, and $B = (2^n - D)/(2^n - 1)$ if they are distinct (we assume distinct plaintext in the rest of this attack).

When using a single linear hull with empirical ELP, the correlations for the right and wrong keys follow normal distributions with parameters:

$$\begin{aligned} \mu_R &= 0, & \sigma_R^2 &= B/D + \mathrm{ELP}, \\ \mu_W &= 0, & \sigma_W^2 &= B/D + 2^{-n}. \end{aligned}$$

The distributions are both centered on zero, and the variance for the right key is greater. Then, we can sort the keys according to the absolute value of the measured correlation, and expect a larger value for the right key than for the wrong key. More precisely, using a threshold $s = \sigma_W \Phi^{-1}\left(1 - 2^{-a-1}\right)$ on the absolute value of the correlation, the success probability is given by [24, Theorem 2]:

$$P_S = 2 - 2\Phi\left(\frac{\sigma_W}{\sigma_R}\Phi^{-1}\left(1 - 2^{-a-1}\right)\right),$$

where a denotes the advantage of the attack, and Φ is the cumulative distribution function of the standard normal distribution, respectively.

6.3 Attack Parameters

We compute the attack parameters against different variants of SIMON and summarize in Table 8. Then, we explain one attack in detail. Due to the rotation invariant of SIMON, we can repeat the attack by using the rotated distinguisher to improve the success probability, according to [9]. We expect the attack to succeed after $\frac{1}{P_S}$ attempts with average time complexity $C_1 \times \frac{1}{P_S}$, where C_1 is the time complexity to run a single time. To estimate the success probability with a binomial distribution, we have the success probability after $\frac{1}{P_S}$ attempts is $1 - (1 - P_S)^{\frac{1}{P_S}}$.

Key recovery attack on 26-round SIMON48/72. We apply the FWT approach to SIMON48/72, with the 17-round linear approximation $(\{23\}, \emptyset) \rightarrow (\emptyset, \{23\})$ with capacity $2^{-45.19}$, and add five rounds before the distinguisher and four rounds after. Following [9, Algorithm 3], $x_{23}^{(6)}$ can be computed from $\kappa_p = 29$ bits of P, $\kappa_p = 29$ bits of the whitening key $k^{(0)}||k^{(1)}$, and $\kappa_f = 7$ additional key bits. Similarly, $x_{23}^{(r-4)}$ can be computed from $\kappa_c = 16$ bits of C, $\kappa_c = 16$ bits of the whitening key $k^{(r-1)}||k^{(r-2)}$, and $\kappa_b = 2$ additional key bits:

$$\begin{aligned} k_p &= k^{(0)}_{[22,21,20,19,\ldots,9,7,5,4,3]}, k^{(1)}_{[23,22,20,19,18,15,13,12,11,6,5]} \\ k_f &= k^{(2)}_{[21,20,14,13,7]}, k^{(3)}_{[22,15]} \\ k_b &= k^{(r-3)}_{[22,15]} \\ k_c &= k^{(r-2)}_{[21,20,14,13,7]}, k^{(r-1)}_{[23,22,20,19,18,15,13,12,11,6,5]} \end{aligned}$$

We ignore bits that have a linear effect because they only flip the sign of the imbalance. The attack is decomposed in three phases:

Distillation Phase. Compute $\phi(x, y) = \#\{P, C : \chi_p(P) = x, \chi_c(C) = y\}$ for $0 \leq x < 2^{\kappa_p}, 0 \leq y < 2^{\kappa_c}$.

This step only requires setting up $2^{\kappa_p + \kappa_c}$ counters and to iterate over the D available plaintext/ciphertext pairs.

Analysis Phase. For each k_f, k_b, compute $\psi_{\kappa_f,\kappa_b}(x, y) = (-1)^{f(\kappa_f,x) \oplus g(\kappa_b,y)}$ for $0 \leq x < 2^{\kappa_p}, 0 \leq y < 2^{\kappa_c}$, then evaluate the convolution $\left(\phi * \psi_{\kappa_f,\kappa_b}\right)$ using the Fast Walsh Transform.

For each κ_f, κ_b, this requires $2^{\kappa_p+\kappa_c}$ evaluations of f and g to generate ψ_{κ_f,κ_b}, and $3(k_p + k_c) \cdot 2^{\kappa_p+\kappa_c}$ additions and $2^{\kappa_p+\kappa_c}$ multiplications to evaluate the convolution, according to [23]. Assuming that the cost of $\kappa_p + \kappa_c$ additions and the cost of multiplication are comparable to the cost of one encryption, the total complexity of the analysis phase is $\mathcal{O}(2^{\kappa_g})$ using a memory of size $2^{\kappa_p+\kappa_c}$.

Search Phase. For all keys with $q(k_p, k_f, k_b, k_c) \geq s$, exhaustively try all master keys corresponding to the subkey candidates. Due to the linear key schedule of SIMON, we can reconstruct the master key from the $2^{\kappa_g - a}$ candidates using linear algebra. With a threshold $s = F_W^{-1}(1 - 2^{-a})$, we expect a fraction 2^{-a} of the keys to remain. Then, we exhaustively search the remaining key bits, with a complexity of $2^{\kappa_g - a} \times 2^{\kappa - \kappa_g} = 2^{\kappa - a} \approx 2^{72-a}$.

Using the Walsh transform pruning technique of [23] (and partially precomputing the Walsh transform of ψ), the complexity of the analysis phase is reduced to[2]:

$$\begin{aligned} &\rho_A\left(\kappa_p + \kappa_c\right)2^{\kappa_p+\kappa_c} + 2\rho_M 2^{\kappa_p+\kappa_f+\kappa_b+\kappa_c-l_{12}} \\ &+ \rho_A 2^{\kappa_f+\kappa_b+\kappa_c-l_{12}}\left(2^{\kappa_p} + \left(\kappa_p - l_0 - 1\right)2^{\kappa_p-l_0}\right) \\ &+ \rho_A 2^{\kappa_p-l_0+\kappa_f+\kappa_b-l_{12}}\left(2^{\kappa_c} + \left(\kappa_c - l_3 - 1\right)2^{\kappa_c-l_3}\right) \\ &= 45\rho_A 2^{45} + 2\rho_M 2^{54} + \rho_A 2^{25}(2^{29} + 27 \times 2^{28}) \\ &+ \rho_A 2^{38}(2^{16} + 15 \times 2^{16}) \approx 2\rho_M 2^{54}, \end{aligned}$$

with ρ_A the cost of an addition, and ρ_M the cost of a multiplication. Assuming that two multiplications correspond to roughly one evaluation of the cipher, we end up with a complexity of 2^{κ_g}. This variant uses a memory of $2^{\kappa_p+\kappa_c} + 2^{\kappa_p+\kappa_f} + 2^{\kappa_c+\kappa_b} = 2^{45} + 2^{36} + 2^{18} \approx 2^{45}$ elements.

Following the above attack parameter, we obtain the complexity of the analysis phase is 2^{54}. With an advantage of $a = 10$, the complexity of the search phase is 2^{62}, and the success probability $P_S = 0.12$. After $\frac{1}{P_S} = 8.3$ attempts, the success probability is $1 - (1 - P_S)^{\frac{1}{P_S}} \approx 66\%$, and the average time complexity of this attack is $2^{65.06}$.

7 Discussion and Perspective

As shown in Fig.1, we observe that the DW of the SIMECK32 is almost the same as the SW. For better compare DW to SW, we also evaluated other SIMON-like ciphers with different rotate constant.

SIMON-like ciphers with different rotate constant. In Crypto 2015, Kölbl *et al.* explored SIMON-like ciphers with different rotation constants. After the analysis of the diffusion, differential, and linear properties of these ciphers, they screened three candidate rotation constants: $(12, 5, 3)$, $(1, 0, 2)$, and $(7, 0, 2)$. Next, we will call the cipher with rotation constants

[2] With the notation adopted by [23], we have $k_0 = 29, k_1 = 7, k_2 = 2, k_3 = 16, l_{12} = 0, l_0 = 1, l_3 = 0$.

TABLE 8
Attack parameters for linear attacks on SIMON with advantage $a = 10$, $D = 2^{n-1}$. All the attacks used the distinguishers in Table 1.

Variant	Rounds	Source	Search Time	$\kappa_p, \kappa_f, \kappa_b, \kappa_c$	Capacity	C_1	P_S	Time	P
48/72	26=5+17+4	17-bit DW	138.4h	29,7,2,16	$2^{-45.19}$	$2^{54} + 2^{62}$	0.12	$2^{65.06}$	66%
48/96	27=5+17+5	17-bit DW		29,7,7,29	$2^{-45.19}$	$2^{72} + 2^{86}$	0.12	$2^{89.05}$	66%
64/96	32=5+23+4	17-bit DW	140.4h	43,10,2,24	$2^{-60.24}$	$2^{79} + 2^{86}$	0.24	$2^{88.10}$	68%
64/128	33=5+23+5	17-bit DW		43,10,10,43	$2^{-60.24}$	$2^{106} + 2^{118}$	0.24	$2^{120.09}$	68%
96/96	44=5+34+5	17-bit DW	278.6h	30,7,9,38	$2^{-93.74}$	$2^{84} + 2^{86}$	0.07	$2^{90.09}$	65%
96/144	45=6+33+6	17-bit DW		47,18,18,47	$2^{-91.74}$	$2^{130} + 2^{134}$	0.31	$2^{135.77}$	70%
128/128	53=5+43+5	17-bit DW	348.6h	47,14,12,43	$2^{-124.59}$	$2^{116} + 2^{118}$	0.19	$2^{120.72}$	67%
128/256	56=6+43+7	17-bit DW		64,33,55,78	$2^{-124.59}$	$2^{230} + 2^{246}$	0.19	$2^{248.40}$	67%

Search Time: the time of searching linear hull utilized in the attack;
C_1: the time complexity to run the attack a single time;
P_S: success probability to run the attack a single time;
Time= $C_1 \times \frac{1}{P_S}$: the average time by assuming that the attack is repeated $\frac{1}{P_S}$ times;
P: success probability after $\frac{1}{P_S}$ attempts.

TABLE 9
Probability of a 17-round differential $(\emptyset, \{0\}) \rightarrow (\{0\}, \emptyset)$ evaluated under different windows for SIMON48$_{(12,5,3)}$ and SIMON48$_{(7,0,2)}$.

SIMON48$n_{(12,5,3)}$

w-bit	9	10	11	12	13	14	15	16	17
EDP(SW)	-inf	-inf	-inf	-inf	-66.89	-66.49	-64.63	-59.89	-59.65
EDP(DW)	-inf	-inf	-48.13	-47.47	-47.34	-47.14	-47.02	-46.91	-45.99

SIMON48$n_{(7,0,2)}$

w-bit	9	10	11	12	13	14	15	16	17
EDP(SW)	-inf	-inf	-inf	-inf	-51.95	-50.70	-49.05	-48.10	-47.62
EDP(DW)	-inf	-inf	-50.86	-49.01	-48.78	-47.75	-47.48	-46.70	-46.26

(a, b, c) and block size n as SIMON$n_{(a,b,c)}$. To further compare DW with SW, we show in Table 9 the probability of the 17-round differential $(\emptyset, \{0\})$ to $(\{0\}, \emptyset)$ for SIMON48$_{(12,5,3)}$ and SIMON48$_{(7,0,2)}$ for different window sizes. Whatsmore, for the variant SIMON$n_{(1,0,2)}$, which can not be evaluated by SW due to the rotation constant ($c > a, b$), DW can adjust the output difference or mask and trace the diffusion of the input to solve this problem.

Finally, for SIMON48$_{(1,0,2)}$, we rotate the output difference of the left branch to $(1 << ((r-1) \times 2)\% \frac{n}{2})$ and get a 19-round differential $(\emptyset, \{0\})$ to $(\{12\}, \emptyset)$ with EDP $2^{-43.13}$. We also get a 21-round differential $(\emptyset, \{0\})$ to $(\{16\}, \emptyset)$ with EDP $2^{-47.54}$. Impressively, we observe that the advantage of DW over SW is more significant when applied to large rotation constants $(12, 5, 3)$. Compared to SW, DW better exploits the diffusion property of the cipher and guarantees the minimal loss of trails in the first few rounds.

Compared to Dinur et al.'s work [26]. Recently, Dinur *et al.* proposed new, faster generic black-box algorithms for finding certain statistical properties (high-probability differentials, linear biases, boomerangs) in block ciphers [26]. All algorithms are based on "surrogate differentiation". According to [26, Table 1], the time complexity of finding the differential with EDP $\geq p$ is bounded by $\tilde{\mathcal{O}}(2^{n/2}p^{-1})$ costing memory $\tilde{\mathcal{O}}(2^{n/2}p^{-1})$. They also presented a memoryless version, while time complexity is increased to $\tilde{\mathcal{O}}(2^{n/2}p^{-2})$.

When applied to SIMON-like ciphers, our DW methodology exhibits several benefits over the technique presented in [26]:

1) **DW can detect low probability distinguisher.** The algorithm presented in [26, Algorithm 1] relies on a probability testing mechanism that is less adept at identifying low probability distinguishers due to a large amount of required data complexity.
2) **DW can find a key recovery friendly distinguisher.** When applied to SIMON-like ciphers, a distinguisher with low hamming weight input-output can mount a longer key recovery attack due to fewer key candidates. In [26], they detect all differential with probability greater than p, which may cause an unsatisfied distinguisher.
3) **DW has a constant growth in time complexity.** Furthermore, the time complexity of our approach is solely dependent on the window size w, and as demonstrated in Fig. 4, a small w suffices to achieve satisfactory accuracy. For variants with larger block sizes, the time complexity of the method proposed in [26] enlarges exponents due to the increased value of n and the decreased probability p. In contrast, the growth in complexity of our method is constant, due to the extended number of rounds r.

With high applicability, the methods developed by Dinur *et al.* are well-suited for constructing Differential Distribution Tables (DDT), Linear Approximation Tables (LAT), and Boomerang Connectivity Tables (BCT) of large Sbox. When applying dataset experiments, these structures are more likely to be revealed due to higher probability/correlation.

Application to other kinds of ciphers. For symmetric ciphers with different linear layers, for instance, SPN structures with MDS/almost MDS (Maximum Distance Separable) linear layers or Addition-RX algorithms, further research on the DW approach is required. Even for SIMON-like ciphers with larger rotation constant parameters, their diffusive properties are much weaker than those of SPN ciphers. For example, one active bit causes at most three active ones in each round.

The SPN cipher typically exhibits more rapid diffusion than the SIMON-like cipher, which is also because the latter is designed with an extreme focus on minimal hardware area. For SPN cipher like AES, which utilizes an MDS matrix as the linear layer, full diffusion occurs by the second round. This implies that a significant portion of active bits must be discarded early on with the dynamic window (DW) strategy, which can lead to bad results.

For those with an almost MDS matrix, the DW approach can reduce the searching space of the differential or linear hull. Once the input difference/mask is fixed, we can utilize MLW in section 3.1.1 to narrow the search space by forcing the discarded bits to be zero. Meanwhile, it should be noted that determining a DW for these ciphers is not an easy task. The MLW works around full diffusion round, which means that we need to use LWIM to combine several MLW and form a DW with more rounds. For these ciphers, we believe combining MLW with SAT problems could yield better results, and we defer this task to future work.

8 Conclusion

In this paper, we followed Leurent *et al.*'s framework but adopted a dynamic way of choosing windows for each round. To determine these dynamic windows (DW), we proposed the MLW (minimal loss window) and LMIM (link window in the middle) strategies. In our MLW strategy, the window is chosen to contain all possibly active bits as the number of them is no greater than the window size w. If the number of active bits is greater than w, we heuristically exclude some possibly active bits out of the window and restrict them as zero differences/masks. To maintain a lower loss of trails, these excluded bits are chosen using minimal active probability test. However, the test can only apply to the first few rounds (around the full diffusion). To solve this problem the LWIM strategy is proposed to link two short MLWs and form a full DW. With these two strategies, we obtained the w-bit DW for SIMON and SIMECK. These windows are very different from the SW for SIMON, while being similar to those SW for SIMECK. Benefiting from these dynamic windows, we observed stronger differentials and linear hulls than previously proposed for almost all versions of SIMON. With these stronger distinguishers, we mounted the best key recovery attacks against SIMON. Moreover, we improved the previous analysis results on the small version of SIMON.

Acknowledgments

We thank the anonymous reviewers for their valuable comments and suggestions to improve the quality of the paper. This work is supported by the National Natural Science Foundation of China (Grant No. 62032014), the National Key Research and Development Program of China (Grant No. 2018YFA0704702), the Major Basic Research Project of Natural Science Foundation of Shandong Province, China (Grant No. ZR202010220025).

References

[1] R. Beaulieu, D. Shors, J. Smith, S. Treatman-Clark, B. Weeks, and L. Wingers, "The SIMON and SPECK lightweight block ciphers," in *Proceedings of the 52nd Annual Design Automation Conference, San Francisco, CA, USA, June 7-11, 2015.* ACM, 2015, pp. 175:1–175:6. [Online]. Available: https://doi.org/10.1145/2744769.2747946

[2] F. Abed, E. List, S. Lucks, and J. Wenzel, "Differential cryptanalysis of round-reduced simon and speck," in *Fast Software Encryption - 21st International Workshop, FSE 2014, London, UK, March 3-5, 2014. Revised Selected Papers*, ser. Lecture Notes in Computer Science, C. Cid and C. Rechberger, Eds., vol. 8540. Springer, 2014, pp. 525–545. [Online]. Available: https://doi.org/10.1007/978-3-662-46706-0_27

[3] A. Biryukov, A. Roy, and V. Velichkov, "Differential analysis of block ciphers SIMON and SPECK," in *Fast Software Encryption - 21st International Workshop, FSE 2014, London, UK, March 3-5, 2014. Revised Selected Papers*, ser. Lecture Notes in Computer Science, C. Cid and C. Rechberger, Eds., vol. 8540. Springer, 2014, pp. 546–570. [Online]. Available: https://doi.org/10.1007/978-3-662-46706-0_28

[4] H. Chen and X. Wang, "Improved linear hull attack on round-reduced simon with dynamic key-guessing techniques," in *Fast Software Encryption - 23rd International Conference, FSE 2016, Bochum, Germany, March 20-23, 2016, Revised Selected Papers*, ser. Lecture Notes in Computer Science, T. Peyrin, Ed., vol. 9783. Springer, 2016, pp. 428–449. [Online]. Available: https://doi.org/10.1007/978-3-662-52993-5_22

[5] S. Kölbl, G. Leander, and T. Tiessen, "Observations on the SIMON block cipher family," in *Advances in Cryptology - CRYPTO 2015 - 35th Annual Cryptology Conference, Santa Barbara, CA, USA, August 16-20, 2015, Proceedings, Part I*, ser. Lecture Notes in Computer Science, R. Gennaro and M. Robshaw, Eds., vol. 9215. Springer, 2015, pp. 161–185. [Online]. Available: https://doi.org/10.1007/978-3-662-47989-6_8

[6] S. Kölbl and A. Roy, "A brief comparison of simon and simeck," in *Lightweight Cryptography for Security and Privacy - 5th International Workshop, LightSec 2016, Aksaray, Turkey, September 21-22, 2016, Revised Selected Papers*, ser. Lecture Notes in Computer Science, A. Bogdanov, Ed., vol. 10098. Springer, 2016, pp. 69–88. [Online]. Available: https://doi.org/10.1007/978-3-319-55714-4_6

[7] Z. Liu, Y. Li, and M. Wang, "Optimal differential trails in simon-like ciphers," *IACR Trans. Symmetric Cryptol.*, vol. 2017, no. 1, pp. 358–379, 2017. [Online]. Available: https://doi.org/10.13154/tosc.v2017.i1.358-379

[8] X. Wang, B. Wu, L. Hou, and D. Lin, "Automatic search for related-key differential trails in simon-like block ciphers based on MILP," in *Information Security - 21st International Conference, ISC 2018, Guildford, UK, September 9-12, 2018, Proceedings*, ser. Lecture Notes in Computer Science, L. Chen, M. Manulis, and S. A. Schneider, Eds., vol. 11060. Springer, 2018, pp. 116–131. [Online]. Available: https://doi.org/10.1007/978-3-319-99136-8_7

[9] G. Leurent, C. Pernot, and A. Schrottenloher, "Clustering effect in simon and simeck," in *Advances in Cryptology - ASIACRYPT 2021 - 27th International Conference on the Theory and Application of Cryptology and Information Security, Singapore, December 6-10, 2021, Proceedings, Part I*, ser. Lecture Notes in Computer Science, M. Tibouchi and H. Wang, Eds., vol. 13090. Springer, 2021, pp. 272–302. [Online]. Available: https://doi.org/10.1007/978-3-030-92062-3_10

[10] G. Yang, B. Zhu, V. Suder, M. D. Aagaard, and G. Gong, "The simeck family of lightweight block ciphers," in *Cryptographic Hardware and Embedded Systems - CHES 2015 - 17th International Workshop, Saint-Malo, France, September 13-16, 2015, Proceedings*, ser. Lecture Notes in Computer Science, T. Güneysu and H. Handschuh, Eds., vol. 9293. Springer, 2015, pp. 307–329. [Online]. Available: https://doi.org/10.1007/978-3-662-48324-4_16

[11] S. Sun, L. Hu, M. Wang, P. Wang, K. Qiao, X. Ma, D. Shi, L. Song, and K. Fu, "Towards finding the best characteristics of some bit-oriented block ciphers and automatic enumeration of (related-key) differential and linear characteristics with predefined properties," *IACR Cryptol. ePrint Arch.*, p. 747, 2014. [Online]. Available: http://eprint.iacr.org/2014/747

[12] M. A. Abdelraheem, J. Alizadeh, H. A. Alkhzaimi, M. R. Aref, N. Bagheri, P. Gauravaram, and M. M. Lauridsen, "Improved linear cryptanalysis of reduced-round simon," *IACR Cryptol. ePrint Arch.*, p. 681, 2014. [Online]. Available: http://eprint.iacr.org/2014/681

[13] N. Wang, X. Wang, K. Jia, and J. Zhao, "Differential attacks on reduced SIMON versions with dynamic key-guessing techniques," *Sci. China Inf. Sci.*, vol. 61, no. 9, pp. 098 103:1–098 103:3, 2018. [Online]. Available: https://doi.org/10.1007/s11432-017-9231-5

[14] K. Qiao, L. Hu, and S. Sun, "Differential security evaluation of simeck with dynamic key-guessing techniques," in *Proceedings of the 2nd International Conference on Information Systems Security and Privacy, ICISSP 2016, Rome, Italy, February 19-21, 2016*, O. Camp, S. Furnell, and P. Mori, Eds. SciTePress, 2016, pp. 74–84. [Online]. Available: https://doi.org/10.5220/0005684400740084

[15] L. Qin, H. Chen, and X. Wang, "Linear hull attack on round-reduced simeck with dynamic key-guessing techniques," in *Information Security and Privacy - 21st Australasian Conference, ACISP 2016, Melbourne, VIC, Australia, July 4-6, 2016, Proceedings, Part II*, ser. Lecture Notes in Computer Science, J. K. Liu and R. Steinfeld, Eds., vol. 9723. Springer, 2016, pp. 409–424. [Online]. Available: https://doi.org/10.1007/978-3-319-40367-0_26

[16] R. Beaulieu, D. Shors, J. Smith, S. Treatman-Clark, B. Weeks, and L. Wingers, "The SIMON and SPECK families of lightweight block ciphers," *IACR Cryptol. ePrint Arch.*, p. 404, 2013. [Online]. Available: http://eprint.iacr.org/2013/404

[17] K. Nyberg, "Linear approximation of block ciphers," in *Advances in Cryptology - EUROCRYPT '94, Workshop on the Theory and Application of Cryptographic Techniques, Perugia, Italy, May 9-12, 1994, Proceedings*, ser. Lecture Notes in Computer Science, vol. 950. Springer, 1994, pp. 439–444.

[18] J. Alizadeh, H. AlKhzaimi, M. R. Aref, N. Bagheri, P. Gauravaram, A. Kumar, M. M. Lauridsen, and S. K. Sanadhya, "Cryptanalysis of SIMON variants with connections," in *Radio Frequency Identification: Security and Privacy Issues - 10th International Workshop, RFIDSec 2014, Oxford, UK, July 21-23, 2014, Revised Selected Papers*, ser. Lecture Notes in Computer Science, N. Saxena and A. Sadeghi, Eds., vol. 8651. Springer, 2014, pp. 90–107. [Online]. Available: https://doi.org/10.1007/978-3-319-13066-8_6

[19] C. Blondeau and K. Nyberg, "New links between differential and linear cryptanalysis," in *Advances in Cryptology - EUROCRYPT 2013, 32nd Annual International Conference on the Theory and Applications of Cryptographic Techniques, Athens, Greece, May 26-30, 2013. Proceedings*, ser. Lecture Notes in Computer Science, T. Johansson and P. Q. Nguyen, Eds., vol. 7881. Springer, 2013, pp. 388–404. [Online]. Available: https://doi.org/10.1007/978-3-642-38348-9_24

[20] A. Bogdanov, L. R. Knudsen, G. Leander, C. Paar, A. Poschmann, M. J. B. Robshaw, Y. Seurin, and C. Vikkelsoe, "PRESENT: an ultra-lightweight block cipher," in *Cryptographic Hardware and Embedded Systems - CHES 2007, 9th International Workshop, Vienna, Austria, September 10-13, 2007, Proceedings*, ser. Lecture Notes in Computer Science, P. Paillier and I. Verbauwhede, Eds., vol. 4727. Springer, 2007, pp. 450–466. [Online]. Available: https://doi.org/10.1007/978-3-540-74735-2_31

[21] M. Matsui, "Linear cryptanalysis method for DES cipher," in *Advances in Cryptology - EUROCRYPT '93, Workshop on the Theory and Application of of Cryptographic Techniques, Lofthus, Norway, May 23-27, 1993, Proceedings*, ser. Lecture Notes in Computer Science, T. Helleseth, Ed., vol. 765. Springer, 1993, pp. 386–397. [Online]. Available: https://doi.org/10.1007/3-540-48285-7_33

[22] B. Collard, F. Standaert, and J. Quisquater, "Improving the time complexity of matsui's linear cryptanalysis," in *Information Security and Cryptology - ICISC 2007, 10th International Conference, Seoul, Korea, November 29-30, 2007, Proceedings*, ser. Lecture Notes in Computer Science, K. Nam and G. Rhee, Eds., vol. 4817. Springer, 2007, pp. 77–88. [Online]. Available: https://doi.org/10.1007/978-3-540-76788-6_7

[23] A. Flórez-Gutiérrez and M. Naya-Plasencia, "Improving key-recovery in linear attacks: Application to 28-round PRESENT," in *Advances in Cryptology - EUROCRYPT 2020 - 39th Annual International Conference on the Theory and Applications of Cryptographic Techniques, Zagreb, Croatia, May 10-14, 2020, Proceedings, Part I*, ser. Lecture Notes in Computer Science, A. Canteaut and Y. Ishai, Eds., vol. 12105. Springer, 2020, pp. 221–249. [Online]. Available: https://doi.org/10.1007/978-3-030-45721-1_9

[24] C. Blondeau and K. Nyberg, "Improved parameter estimates for correlation and capacity deviates in linear cryptanalysis," *IACR Trans. Symmetric Cryptol.*, vol. 2016, no. 2, pp. 162–191, 2016. [Online]. Available: https://doi.org/10.13154/tosc.v2016.i2.162-191

[25] ——, "Joint data and key distribution of simple, multiple, and multidimensional linear cryptanalysis test statistic and its impact to data complexity," *Des. Codes Cryptogr.*, vol. 82, no. 1-2, pp. 319–349, 2017. [Online]. Available: https://doi.org/10.1007/s10623-016-0268-6

[26] I. Dinur, O. Dunkelman, N. Keller, E. Ronen, and A. Shamir, "Efficient detection of high probability statistical properties of cryptosystems via surrogate differentiation," Cryptology ePrint Archive, Paper 2023/288, 2023, https://eprint.iacr.org/2023/288. [Online]. Available: https://eprint.iacr.org/2023/288

Chao Niu received the BE degree from the University of Electronic Science and Technology of China. He received the PhD in Cyberspace Security at Shandong University. His current research focuses on the analysis of symmetric key algorithms.

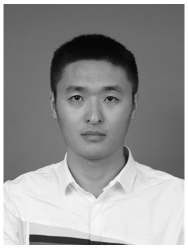

Muzhou Li received the BS degree from Shandong University, where he received the PhD in Cyberspace Security. He is working as a Post-doctoral at Shandong University. His research interest is cryptography, including the design and analysis of symmetric-key algorithms.

Jifu Zhang received the BS degree and MS degree from Shandong University in Information Security and Cyberspace Security, respectively. He is currently working at Huawei Technologies. His research interest is information security.

Meiqin Wang received the BS and MS degree from Xi'an Jiaotong University, in 1996 and 1999, respectively, and PhD degree from Shandong University, in 2007. She was a guest researcher of The University of Hong Kong, in 2005 and 2008, and guest researcher of KU Leuven, from 2010 to 2011. She is currently a professor with the School of Cyber Science and Technology, Shandong University. She has coauthored more than 100 research peer reviewed journal and conference papers. She was the General Co-Chair of FSE 2023. Her research interest is cryptography, including the design and analysis of symmetric-key algorithms.